

ated pulses and the target voltages were monitored using a Tectronix voltage probe and Digital Phosphor Oscilloscope as shown in Figure 1. A schematic of the experimental set-up for the optical emission detection is shown in Figure 2.

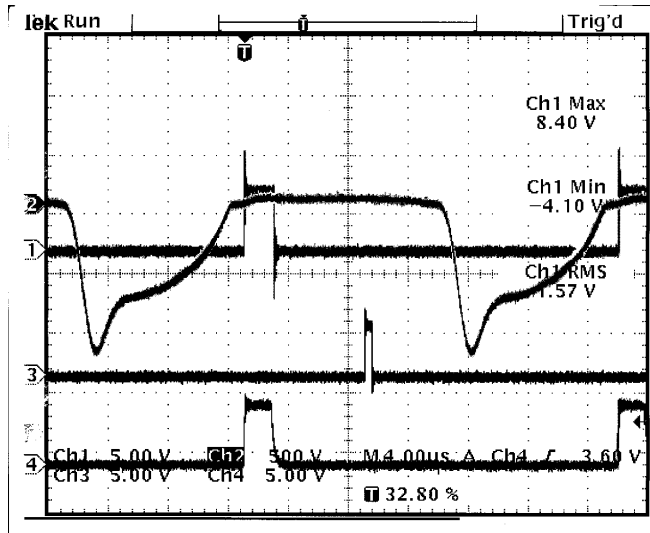


Figure 1: Oscilloscope traces of the target power (trace 2), the TTL pulse from the target (trace 1), and the pulse from the pulse and delay generator (trace 3).

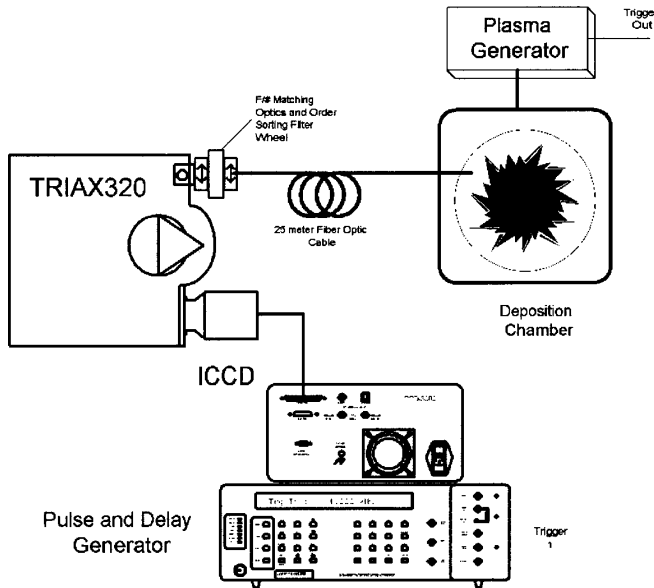


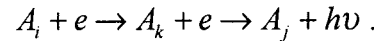
Figure 2: Optical emission detection scheme.

OPTICAL EMISSION

The emission lines chosen for this investigation were the argon lines located at 750 and 751 nm. These lines were chosen for several reasons. Argon gas is the main component of the sputtering processes and present in large enough quantities to get sufficient emission intensity. The close proximity

of the two lines means that the grating efficiencies for each line should be nearly identical and can be monitored simultaneously. Both lines have branching ratios of one, meaning that all atoms in the excited state are relaxed into only one level, generating only one emission wavelength. Furthermore, the contribution of metastables to these two excited states has been shown to be very small [5,6] and their effects are therefore neglected.

The quantities that effect emission probabilities can be expressed in the following equations. For excitation of a rare gas such as argon from its ground or lower state A_i to an excited state A_k with spontaneous relaxation to a lower state A_j , we have (shown schematically in Figure 3):



The intensity of the resulting emission, is expressed by [7]:

$$I_{A_i,j,k} = 4\pi\alpha(\lambda_{j,k})n_{A_i}Q_k b_{j,k} \int_{v_{0,A_i,k}}^{\infty} \sigma_{A_i,k}(v)v^3 f_e(v)dv , \quad (1)$$

where $\alpha(\lambda_{j,k})$ is the spectrometer sensitivity for the emission wavelength, n_{A_i} is the number density of the atom in its initial state, and $\sigma_{A_i,k}(v)$ is the effective electron impact cross section from level A_k at electron speed v . The quantum yield for the emission of a photon upon relaxation, Q_k , for atoms is given by:

$$Q_k = \frac{\tau^{-1}}{\tau^{-1} + k_q P} , \quad (2)$$

where τ is the radiative lifetime of the atom and k_q is the effective quenching rate constant for A_k by all species at pressure P . The symbol $f_e(v)$ refers to the electron distribution function (we assume for comparison that it is Maxwellian, but the equation is not defined by a Maxwellian distribution), and $b_{j,k}$ is the branching ratio of the emissive state (the amount of emission from state j going to state k divided by all possible emission from state j).

For optical emission experiments, quantitative information is nearly impossible to obtain. However, a great deal of information can be obtained by measuring relative emission intensities. For these experiments, because the two wavelengths monitored are so close in energy, we assume that the grating sensitivities to these two wavelengths are identical. Sensitivities of individual CCD pixels are within 10%, but because a large number of CCD elements are used for each peak measured, it is assumed that these variations become cumulatively negligible. We therefore assume the quantity $\alpha(\lambda_{j,k})$ to be identical for both wavelengths. Because both emission lines are observed under the same conditions, it is clear that the

quantity n_{A_i} is also identical for both transitions. The quantum yield, Q_k , as expressed in Equation (2), reduces to one due to the low process pressures and short radiative lifetimes of the emitting states. Furthermore, the branching ratios, $b_{j,k}$ for both transitions are both 1, and so all quantities outside the integral of equation (1) cancel.

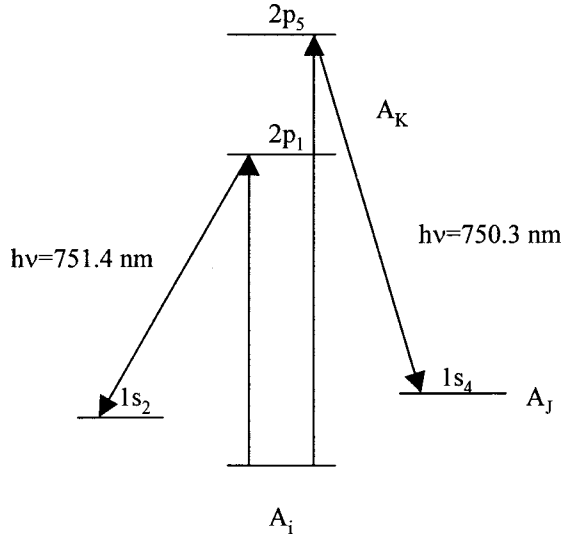


Figure 3: Schematic of the energy level diagram for the 750.4 and 751.4 nm electron impact emission lines of argon.

Electron impact cross sections for argon atoms, $\sigma_{A_i}(\nu)$, were taken from the investigations of Feltsan and Zapesochnyi [8], which provides cross sections through electron temperatures of 100 eV. The electron energy distribution was assumed to be Maxwellian, according to the expression:

$$f_e(\nu) = \left(\frac{m_e}{2\pi k T_e} \right)^{3/2} \exp\left(-\frac{m_e \nu^2}{2k T_e} \right). \quad (3)$$

where m_e is the electron mass, and T_e is the Maxwellian electron temperature. Integrating the product of this expression with the cross section functions, we can obtain a relative probability of emission at a variety of electron temperatures for each transition. This probability should be independent of electron density or number density of argon atoms. Figure 4 shows the predicted relative emission probabilities for both the 750 and 751 nm lines as well as the ratio of these lines at various electron temperatures. These ratios should not be used to determine actual electron temperatures, but only to indicate electron temperature trends. The main feature to note in Figure 4 is that as electron temperatures increase the relative emission probabilities increase, but that increase becomes slower as the electron temperatures get higher.

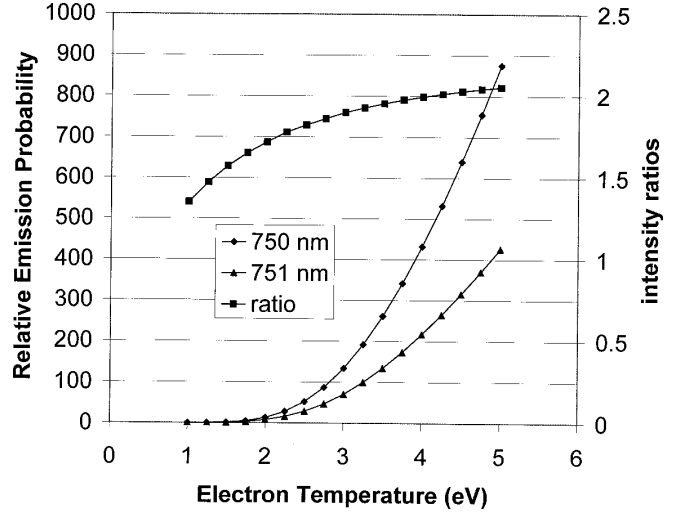


Figure 4: Calculated relative emission probabilities for 750.4 and 751.4 nm transitions, as well as the ratios between them.

MID FREQUENCY PULSED DC PLASMAS

A mid-frequency single-ended asymmetric pulsed DC power supply (Pinnacle Plus ADCAP from Advanced Energy) was used on a reactive sputtering system equipped with rectangular 5" x 25" magnetron cathodes. Frequencies between 20 and 275 kHz were used, and off times varied between 0.6 and 5 μ s. Frequencies and duty cycles investigated were primarily dictated by the ability to sustain a plasma with little detectable arcing. The emission peaks, an example of which can be seen in Figure 5, of both the 750 and 751 nm lines were integrated and the ratio of these intensities was taken by dividing the 750 nm integrated peak intensity, by that of the 751 nm peak.

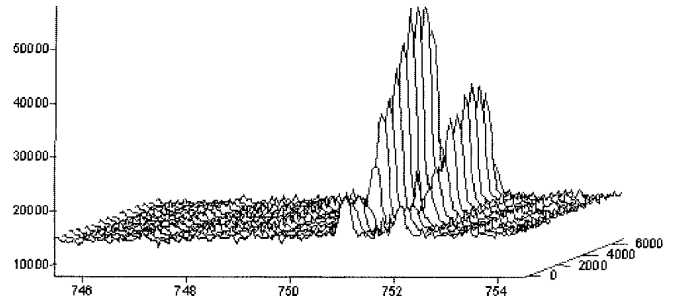


Figure 5: An example of optical emission spectra taken.

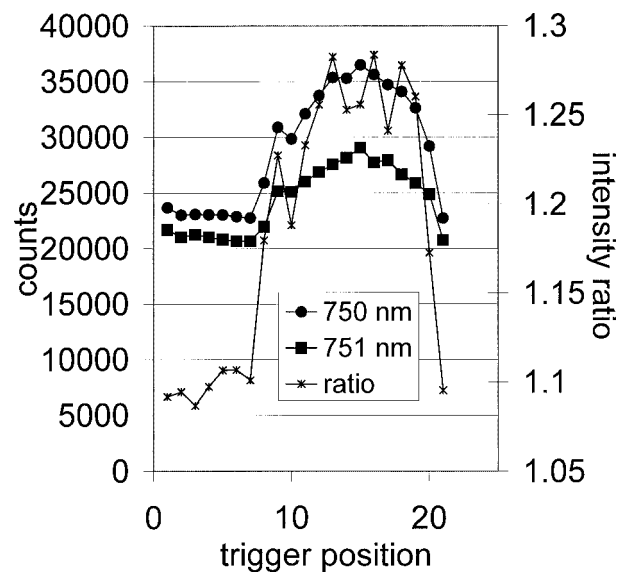
In all cases, the peak ratios increased when the targets were under the high negative voltage that accompanies cathode sputtering, indicating that the electron temperatures increase when the plasma is pulsed on. The degree of this increase is similar for all pulsed systems studied, but a distinct trend can be seen that may indicate pulsing conditions that create slightly higher electron temperatures, and the concomitant better film quality.

In Figure 6a, it can be seen that the emission intensities for both argon lines increase when the pulse is turned on. For all frequencies monitored in this study there is a “double hump” shape to the intensity curves that is also observable on the ratio curves, as can also be seen in Figure 6a. This double hump shape is reflected in the voltage trace from the oscilloscope (seen on Figure 6b), which shows a high “clamping” potential of about -900 V (increasing slightly with increased frequency and decreased off-time up to -1100 V) falling back to a sustained voltage of about -600 V. The clamping voltage becomes the dominant applied potential to the target as the frequency increases until the sustaining voltage is completely absent at about 175 kHz. Thus, all emission spectra show a steep rise over 1 microsecond with a sharp fall and a secondary rise over about 3 microseconds (the period that the clamping potential is held and similar to the thermalization times expected for the electrons in the plasma). The emission then decreases to a constant level if pulse-on time allows (e.g. 2 to 3 more microseconds). As the target voltage shifts to the reverse pulse, within 1 microsecond the emission intensity is back to its off-pulse level.

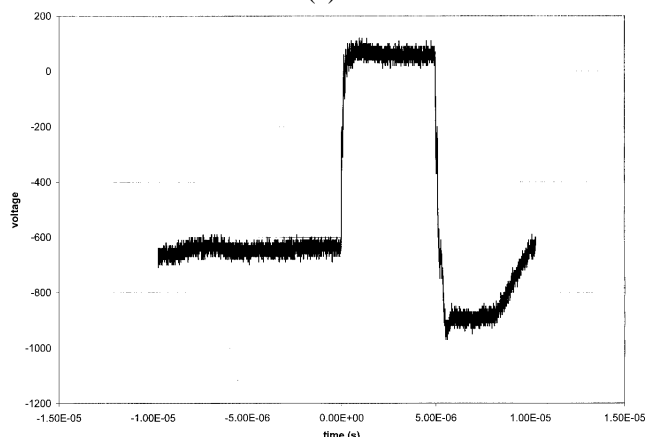
To better understand the emission profiles, higher resolution emission studies were done with 100 ns pulse widths. The data show that the initial upward spike happens over about 200 ns, while the first fall takes about 600 ns at 225 kHz and 200 ns at 100 kHz. The time for the intensity to decrease from the on-pulse values to the off-pulse values was about 400 μ s.

The source of the initial spike in the emission intensity parallels the initial increase in electron temperatures seen in Langmuir probe studies of non-reactive sputtering plasmas by Bradley et al. [9]. They also see an oscillation after the initial spike that they attribute to the properties of the power supply, and acknowledge its affect on the plasma properties.

The hypothesis put forth by Bradley et al. suggests that the rapid formation and expansion of the ion sheath is the primary cause of the initial electron temperature spike. The spike (greater than 20 eV for 50 kHz, and 8 eV for 100 kHz) in their work was attributed to some electrons acquiring the full or partial sheath potential from the abruptly changing applied target voltage.



(a)



(b)

Figure 6: (a) The relative integrated peak emissions of the argon 750.3 and 751.4 nm lines over the pulse width of the plasma. These data were taken at 100 kHz. Data points indicate the start time of the pulse with a 500 ns pulse width. This width allows averaging of all emissions up to the time of the following data point. (b) Oscilloscope trace of target voltage at 150 kHz.

The secondary hump seen in our data is a result of the transition from the clamping to a plasma-sustained voltage or is associated with the thermalization time of the electrons. One notes a rise in emission intensity and ratio over a span of about 3 μ s, the same time period during which the striking voltage is held. Analysis of the ion current to the target measured by a current probe shows that the current increases dramatically as the target is turned on, causing a spike in the current trace in Figure 7. This spike corresponds nicely to the initial increase in optical emission intensity. Within a half of a microsecond, however, the current is seen to level off until

the power supply switches to its sustaining voltage. At this point the current increases when the voltage decreases as would be necessary to meet the constant power conditions.

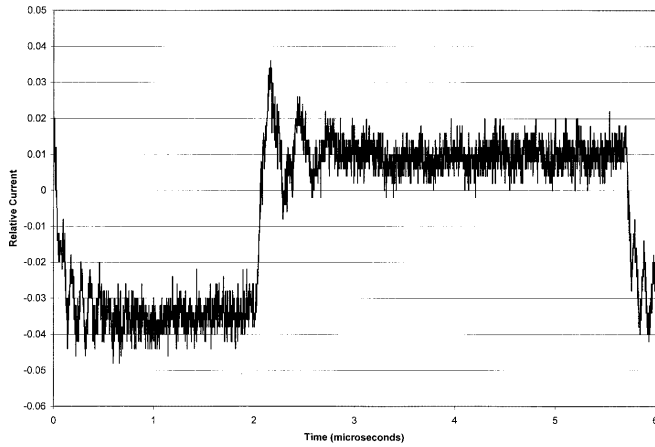


Figure 7: Current trace from the silicon target at 40 kHz, 5 μ s off-time

Table 1 shows the average emission ratios and maximum ratios for all conditions studied. Figure 8 shows these data graphed as a function of frequency only. It can be seen from these data, that pulse-off times have very little effect on the emission properties. Frequency has a complex effect on these properties. There is clearly some error associated with these emission measurements that are increased when ratios are calculated. Some errors can be attributed to the non-uniformity of the plasmas both in space and over small time scales. Other errors may be associated with optical cascade effects.

Table 1: Average and maximum emission ratios for all conditions studied.

<i>frequency</i>	<i>Off-time</i>	<i>avg. ratio</i>	<i>max. ratio</i>
20	5	1.164742	1.222864
40	5	1.171748	1.237775
100	4.5	1.146991	1.210026
100	4.5	1.185216	1.283741
150	2.5	1.16516	1.246124
175	2	1.168873	1.233176
175	1.2	1.174731	1.260676
175	2.6	1.183865	1.267045
225	2	1.176609	1.262275
225	2	1.192985	1.295625
275	1.5	1.157485	1.2118
275	0.6	1.162547	1.202006
275	1.2	1.165144	1.199494

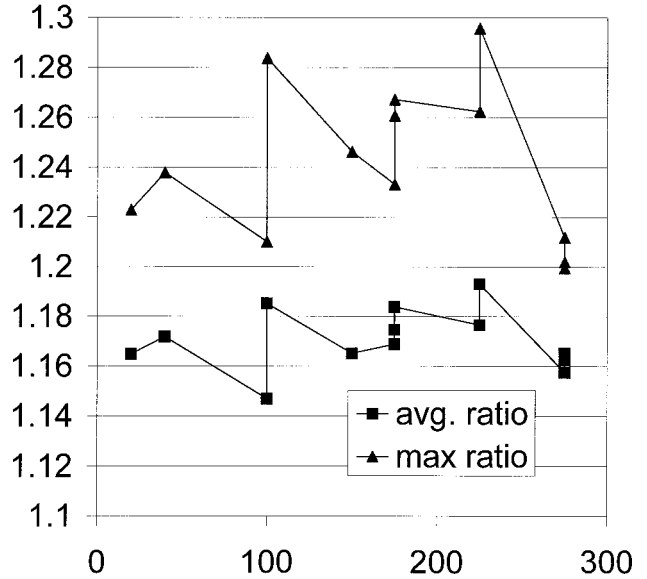


Figure 8: Average and maximum emission ratios for all conditions studied.

AC PLASMA

A PE2 40 kHz AC power supply from Advanced Energy was used on a unbalanced linked dual magnetron cathode sputtering system with 5" x 15" targets. Figure 9 shows the target voltage trace from this power supply as well as the emission and ratio plots. It is very clear that the emission profile follows that of the voltage curve. Of note is the lack of initial high energy spike, presumably due to the lack of the initial large voltage drop and therefore less dramatic sheath acceleration. The maximum emission ratio for the AC process is 1.24 and the average ratio is 1.15. It should be noted, however, that the AC data are taken at a considerably lower power than the DC pulsed data (4 kW versus 6 kW) due to the experimental restrictions mentioned earlier.

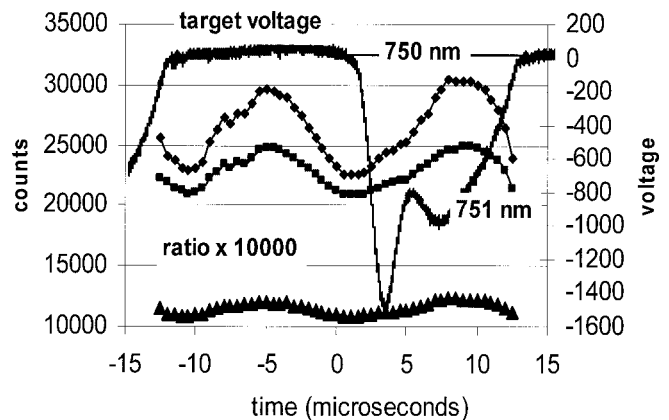
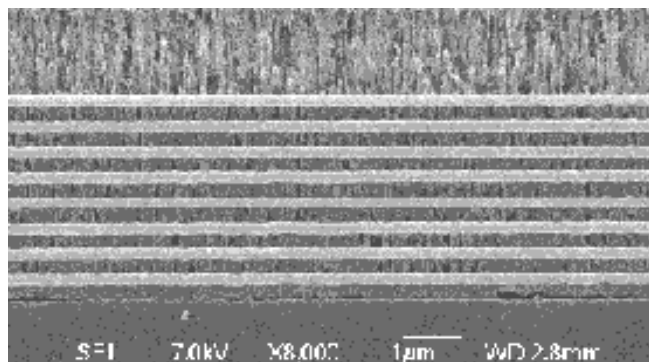


Figure 9: Voltage and emission traces for the 40 kHz AC plasma.

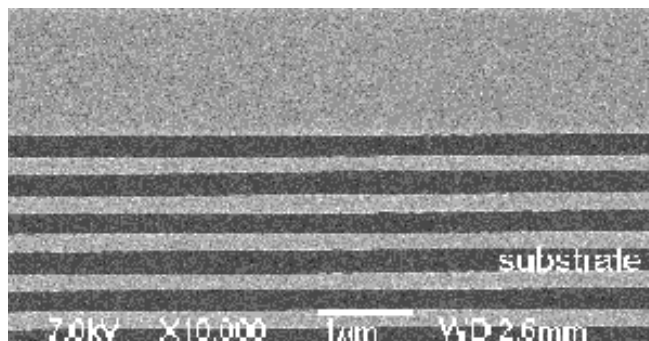
FILM STUDIES

Some very preliminary studies were done on the quality of films deposited under a few of the conditions studied with optical emission. In general, films deposited using the AC process exhibited significantly fewer “splatter” defects due to the fewer arc events in the AC process compared to the pulsed DC processes.

Two different frequencies were used in the DC-pulsed mode to grow single cavity optical films. Figure 10 shows that at 175 kHz (2 μ s off time) films show a vast improvement in interfacial roughness over those grown at 20 kHz (5 μ s off time). This correlates nicely with the higher optical emission intensity ratios in the 175 kHz range compared to that at 20 kHz. Films deposited using the AC process were of higher quality than either DC pulsed frequency. Films were not deposited in the 225 kHz range, where it appears that DC pulsed plasmas obtain higher electron temperatures than the 40 kHz AC process. It seems possible that film qualities may be superior if one used a dual symmetric DC bipolar pulsed process at that frequency rather than using the AC process. This comparison, however, remains for future work.



(a)



(b)

Figure 10: (a) The interface between silica and tantala for films grown at 20 KHz and (b) 175 kHz frequency pulsing.

CONCLUSIONS

We have shown that optical emission can be used to obtain relative time-resolved electron temperatures present in reactive sputtering plasmas. This information could help zero in on the process space most suitable for high quality film growth.

Pulsed DC plasmas exhibit an initial electron temperature spike in the first microsecond of pulse time, followed by a second broader rise and fall influenced by the characteristics of the power supply used. The AC plasmas did not exhibit the initial electron energy spike within the resolution used in our experiments.

There appears to be some frequency dependence on electron temperatures in the pulsed DC system, and further film comparisons done at these different frequencies should shed light on the correlation of the maximum or average electron temperatures to film properties. Higher resolution spectra would help to isolate the peak intensity ratios, which would occur in approximately the first microsecond after the pulse has been turned on. The theoretical shutter time limit for the optical emission apparatus used is 20 ns. The film comparisons and higher resolution studies will be incorporated into future investigations into these systems.

REFERENCES

1. D.A. Glocker, *J. Vac. Sci. Tech. A*, 11(6) pg. 2989, 1993.
2. A. Belkind, A. Freilich, and R. Scholl, “Electrical Dynamics of Pulsed Plasmas”, *39th Annual Technical Conference Proceedings of the Society of Vacuum Coaters*, pg. 321, 1998.
3. P.J. Kelly and R.D. Arnell, *Vacuum*, 56 pg. 159, 2000.
4. L.J. Mahoney, G.W. McDonough, D.C. Carter, G.A. Roche, and H.V. Walde, “Substrate and Plasma Heating with in High Frequency Bi-polar Pulsed Magnetron Sputtering Applications”, *AVS 46th Int’l Symposium*, Seattle, Washington, Oct. 25-29, 1999.
5. V.M. Donnelly, *J. Vac. Sci. Tech. A*, 14 pg. 1076, 1996.
6. M.V. Malyshev and V.M. Donnelly, *J. Vac. Sci. Tech. A*, 15(3) pg. 550, 1997.
7. M.A. Lieberman and A.J. Lichtenberg, *Principles of Plasma Discharges and materials Processing* (Wiley, New York, 1994), pg. 258.
8. P.V. Feltsan and I.P. Zapesochnyi, *Ukr. Fiz. Zh.* 12, 633 (1967).
9. J.W. Bradley, H. Bäcker, P.J. Kelly, and R. D. Arnell, *Surface Coating Technology*, 135/2-3 pg. 221, 2001.